Radiative corrections in measurements of the proton radius.

Igor Akushevich[1] and Alexander Ilyichev[2]

[1] Duke University, Durham, NC USA

[2] Institute for Nuclear Problems, Byelorussian State University, Minsk Belarus

e-mail: igor.akushevich@duke.edu

Introduction

- Measurements of the proton radius based upon lepton scattering experiments allows researchers to reach high measurement precision. However, to achieve this aim,
  - Tight control of systematic uncertainties is necessary.
  - Radiative corrections are the most critical component of these systematic uncertainties.
- In data analyses, the proton radius is estimated through the slope of Q^2-dependence that is estimated using a fitting procedure within the bin-by-bin or Moller-integrated method.
- The objective of this study is to calculate QED radiative corrections and analyze the Q^2-dependence of specific contributions to the total RC in ep and ee-scattering.
- The secondary objective is to identify and review possible ways on how this and other available calculations can be further improved.

The Born and lowest order RC: Feynman graphs

The Born cross section and the lowest order RC are defined by diagrams with emission of the real photon and loop diagrams

The Born matrix element:

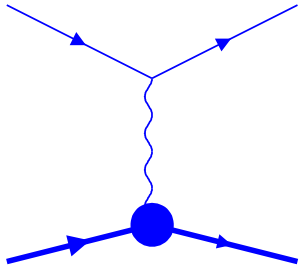

One loop diagrams:

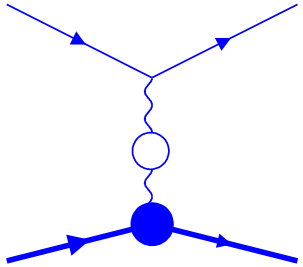

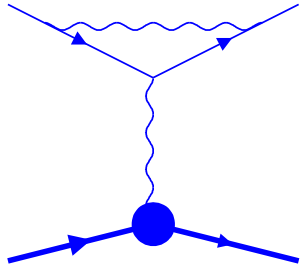

Real photon emission:

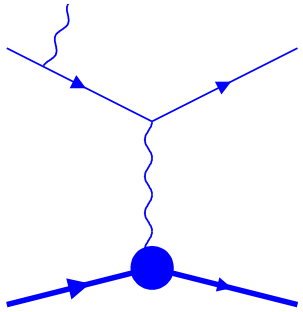

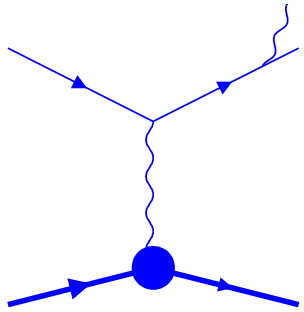

The Born cross section

The Born cross section of unpolarized elastic lp-scattering

$$l(k_1) + p(p_1) \to l'(k_2) + p'(p_2)$$

($k_1^2 = k_2^2 = m^2$, $p_1^2 = p_2^2 = M^2$) is described by the two kinematical invariants:

$$S = 2p_1k_1, \qquad Q^2 = -(k_1 - k_2)^2.$$

and has the form

$$\frac{d\sigma_B}{dQ^2} = \frac{2\pi\alpha^2}{\lambda_S Q^4}\left(\theta_B^1 \mathcal{F}_1(Q^2) + \theta_B^2 \mathcal{F}_2(Q^2)\right),$$

$\lambda_S = S^2 - 4m^2M^2$ and

$$\theta_B^1 = Q^2 - 2m^2, \qquad \theta_B^2 = \frac{S(S - Q^2) - M^2Q^2}{2M^2},$$

$$\mathcal{F}_1 = Q^2G_M^2, \ \mathcal{F}_2 = 4M^2\frac{G_E^2 + \tau_pG_M^2}{1 + \tau_p},$$

Kinematic reqion for Q^2 is (0, Q^2_{max}), where $Q^2_{max} = \lambda_S/(S + M^2 + m^2)$

The lowest order RC: Exact formulae for ep-scattering

$$\frac{d\sigma_{RC}}{dQ^2} = \frac{\alpha}{\pi}(\delta_{IR} + \delta_{\rm vert} + \delta^l_{\rm vac} + \delta^h_{\rm vac})\frac{d\sigma_B}{dQ^2} + \frac{d\sigma_{AMM}}{dQ^2} + \frac{d\sigma_F}{dQ^2}.$$

$$\begin{aligned}
\delta_{IR} + \delta_{\rm vert} &= 2\left((Q^2+2m^2)L_m - 1\right)\log\frac{v_{cut}}{mM} + \frac{1}{2}SL_S + \frac{1}{2}XL_X + S_\phi - 2 \\
&\quad + \left(\frac{3}{2}Q^2 + 4m^2\right)L_m - \frac{Q^2+2m^2}{\sqrt{\lambda_m}}\left(\frac{1}{2}\lambda_m L_m^2 + 2{\rm Li}_2\left[\frac{2\sqrt{\lambda_m}}{Q^2+\sqrt{\lambda_m}}\right] - \frac{\pi^2}{2}\right). \\
\delta^l_{\rm vac} &= \sum_{i=e,\mu,\tau}\delta^i_{\rm vac} = \sum_{i=e,\mu,\tau}\left[\frac{2}{3}(Q^2+2m_i^2)L_m^i - \frac{10}{9} + \frac{8m_i^2}{3Q^2}\left(1 - 2m_i^2 L_m^i\right)\right]. \\
\frac{d\sigma_{AMM}}{dQ^2} &= \frac{\alpha^3 m^2 L_m}{2M^2Q^2\lambda_S}\left[12M^2\mathcal{F}_1(Q^2) - (Q^2+4M^2)\mathcal{F}_2(Q^2)\right],
\end{aligned}$$

where

$$L_S = \frac{1}{\sqrt{\lambda_S}}\log\frac{S+\sqrt{\lambda_S}}{S-\sqrt{\lambda_S}},\ L_X = \frac{1}{\sqrt{\lambda_X}}\log\frac{X+\sqrt{\lambda_X}}{X-\sqrt{\lambda_X}}, L_m = \frac{1}{\sqrt{\lambda_m}}\log\frac{\sqrt{\lambda_m}+Q^2}{\sqrt{\lambda_m}-Q^2}$$

and $\lambda_S = S^2 - 4m^2M^2$, $\lambda_X = (S-Q^2)^2 - 4m^2M^2$, and $\lambda_m = Q^4 - 4m^2Q^2$,

The cross section of real photon emission

The real photon emission in lp-scattering

$$l(k_1) + p(p_1) \to l'(k_2) + p'(p_2) + \gamma(k)$$

requires three additional kinematical variables. We will use:

- $t = -(k_1 - k - k_2)^2$ — true virtual photon momentum
- $v = (p + k_1 - k_2)^2 - M^2$ — inelasticity
- ϕ_k — angle between scattering and photon production planes, i.e., planes defined by vectors ($\mathbf{k}_1$, $\mathbf{k}_2$) and ($\mathbf{q}$, $\mathbf{k}$).

The cross section is

$$\frac{d\sigma_F}{dQ^2} = -\frac{\alpha^3}{2\lambda_S} \int\limits_{t_{min}}^{t_{max}} dt \int\limits_{v_1}^{v_{max}} dv \sum_{i=1}^{2} \left(\frac{\mathcal{F}_i(t)}{t^2} \sum_{j=1}^{k_i} (Q^2 + v - t)^{j-3} \theta_{ij}(v,t) - 4F_{IR}\theta_i^B \frac{\mathcal{F}_i(Q^2)}{(Q^2+v-t)^2 Q^4} \right)$$

This expression is the result of analytic integration in respect of ϕ_k.

The structure of the cross section of real photon emission

$$\frac{d\sigma_F}{dQ^2} = -\frac{\alpha^3}{2\lambda_S}\int_0^{v_{max}} dv \int_{t_{min}}^{t_{max}} dt \sum_{i=1}^{2}\left(\frac{\mathcal{F}_i(t)}{t^2}\sum_{j=1}^{k_i}(Q^2+v-t)^{j-3}\theta_{ij}(v,t) - 4F_{IR}\theta_i^B\frac{\mathcal{F}_i(Q^2)}{(Q^2+v-t)^2Q^4}\right)$$

where $\theta_{ij}(v,t)$ are kinematical coefficients that contains 5 types of terms:

- terms coming from the propagator in the initial state radiation
- terms coming from the propagator in the final state radiation
- terms coming from the squared propagator of the initial state radiation (always multiplied by m^2)
- terms coming from the squared propagator of the final state radiation (also always multiplied by m^2)
- other terms

The approach to extract Q^2-dependence of RC:

The leading Q^2-dependence is:

- The factorized real and virtual part of RC

$$\delta_{IR} + \delta_{\rm vert} = \frac{Q^2}{12m^2}\left[4\log\frac{Q^2\lambda_S}{M^2m^4} + 3 + \frac{2S}{\lambda_S}\left(S - 2(S^2 - 3m^2M^2)L_S\right)\right].$$

- The vacuum polarization by leptons and hadrons

$$\delta^l_{vac} = \frac{2}{15}Q^2\sum_{i=e,\mu,\tau}\frac{1}{m_i^2}$$

- Anomalous magnetic moment

$$\frac{d\sigma_{AMM}}{dQ^2} = -\frac{\alpha M^2Q^2}{\pi S^2}\frac{d\sigma_B}{dQ^2}$$

- Multiple soft photon emission

$$\frac{d\sigma_{obs}}{dQ^2} = \exp\left(\frac{\alpha}{\pi}\delta_{inf}\right)\left[1 + \frac{\alpha}{\pi}(\delta_{IR} - \delta_{inf} + \delta_{\rm vert} + \delta^l_{\rm vac} + \delta^h_{\rm vac})\right]\frac{d\sigma_B}{dQ^2} + \frac{d\sigma_{AMM}}{dQ^2} + \frac{d\sigma_F}{dQ^2}.$$

where $\delta_{inf} = 2\left((Q^2 + 2m^2)L_m - 1\right)\log\frac{v_{max}}{mM} \approx \frac{2Q^2}{3m^2}\log\frac{v_{max}}{mM} = \frac{2Q^2}{3m^2}\left(\log q_m + L_s\right)$

RC due to real photon emission at small Q^2

$$\frac{d\sigma_F}{dQ^2} = -\frac{\alpha^3}{2\lambda_S}\int_0^{v_{max}} dv \int_{t_{min}}^{t_{max}} dt \sum_{i=1}^{2}\left(\frac{\mathcal{F}_i(t)}{t^2}\sum_{j=1}^{k_i}(Q^2+v-t)^{j-3}\theta_{ij}(v,t) - 4F_{IR}\theta_i^B\frac{\mathcal{F}_i(Q^2)}{(Q^2+v-t)^2Q^4}\right)$$

Recall that the formfactor in the area of small t or Q^2 is flat, e.g., the dipole formula

$$G_D(Q^2) = \frac{1}{(1+Q^2/\Lambda^2)^2}$$

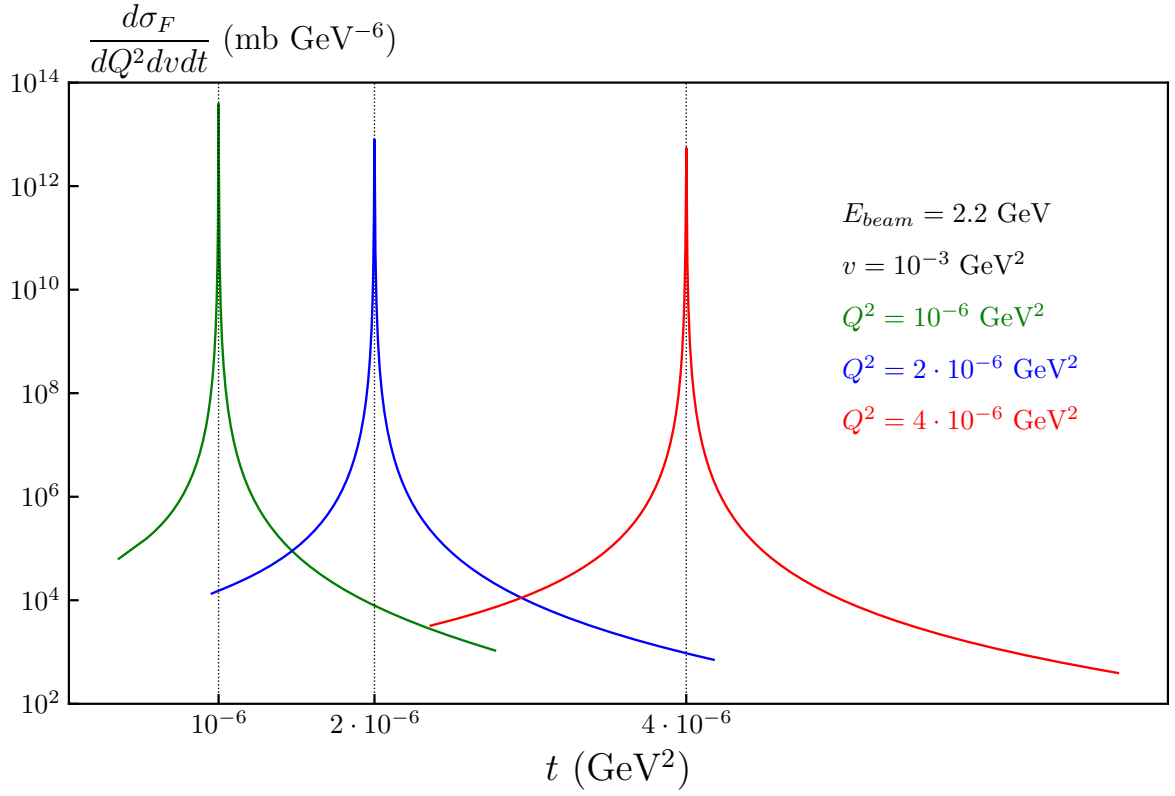

Therefore, the formfactor can be expanded using Tailor series, e.g.,

$$G_E(t) = G_E(Q^2) + (t-Q^2)G'_E(Q^2) + \ldots$$

Details of the calculation

$$\frac{d\sigma_F}{dQ^2} = -\frac{\alpha^3}{2\lambda_S}\int\limits_0^{v_{max}} dv \int\limits_{t_{min}}^{t_{max}} dt\Big(K_1 G_M^2(Q^2) + K_2 G_E^2(Q^2) + \bar{K}_1\big(G_M^2(Q^2)\big)' + \bar{K}_2\big(G_E^2(Q^2)\big)'\Big)$$

- We calculate these integrals analytically.
- To extract an analytic expression for small Q^2 asymptotic, we expand specific contributions by Q^2
- We hold only leading terms by lepton mass in each coefficient, i.e., we expand the exactly calculated integrals within the approximation $Q^2 \ll m^2 \ll S, M^2$ resulting in a series over $q_m = Q/m$

The results are:

- K_2 gives the largest contribution resulting in resulting in $1/Q^2$ behavior of $d\sigma_F/dQ^2$.
- Terms with K_1, $\bar{K}_1$, and $\bar{K}_2$ do not contribute to the cross section in this order.

Details of the calculation

There are four contributions for K_2/Q^8:

- Logarithmic terms from the initial state radiation ($L_s = 2\log(S/(mM))$):

$$q_m^3\left(4q_m - \frac{16}{5}q_m^2 + \frac{25}{9}q_m^3 + L_s(-\frac{16}{3} + 3q_m - \frac{8}{3}q_m^2 + q_m^3)\right)$$

- Logarithmic terms from the final state radiation:

$$L_s q_m^3\left(\frac{16}{3} - 3q_m + \frac{8}{3}q_m^2 - \frac{5}{3}q_m^3\right)$$

- Logarithmic terms from the infrared divergence terms

$$2(2-q_m)q_m^5$$

- Terms not containing logarithms

$$4q_m^4\left(-1 - \frac{1}{5}q_m + \frac{1}{3}q_m^2\right)$$

The sum of these contributions:

$$\left(\frac{19}{9} - \frac{2}{3}L_s\right)q_m^6$$

The terms $O(q_m^3)$, $O(q_m^4)$, and $O(q_m^5)$ completely cancel, resulting in $1/Q^2$ behavior of σ_F.

Numeric example

The cross section can be expressed through the sum of these four contributions:

$$\frac{d\sigma_F}{dQ^2} = \frac{d\sigma_X}{dQ^2} + \frac{d\sigma_S}{dQ^2} + \frac{d\sigma_0}{dQ^2} + \frac{d\sigma_M}{dQ^2}$$

Q^2	$d\sigma_X/dQ^2$	$d\sigma_S/dQ^2$	$d\sigma_0/dQ^2$	$d\sigma_M/dQ^2$	$d\sigma_F/dQ^2$
$1 \cdot 10^{-04}$	$0.32842 \cdot 10^{09}$	$-0.11578 \cdot 10^{09}$	$-0.22115 \cdot 10^{07}$	$-0.85398 \cdot 10^{08}$	$0.12504 \cdot 10^{09}$
$1 \cdot 10^{-05}$	$0.28041 \cdot 10^{11}$	$-0.12323 \cdot 10^{11}$	$0.49904 \cdot 10^{09}$	$-0.53033 \cdot 10^{10}$	$0.10913 \cdot 10^{11}$
$1 \cdot 10^{-06}$	$0.24476 \cdot 10^{13}$	$-0.18985 \cdot 10^{13}$	$0.15947 \cdot 10^{12}$	$-0.25076 \cdot 10^{12}$	$0.45785 \cdot 10^{12}$
$1 \cdot 10^{-07}$	$0.59225 \cdot 10^{15}$	$-0.59265 \cdot 10^{15}$	$0.19813 \cdot 10^{14}$	$-0.95778 \cdot 10^{13}$	$0.98308 \cdot 10^{13}$
$1 \cdot 10^{-08}$	$0.21326 \cdot 10^{18}$	$-0.21475 \cdot 10^{18}$	$0.19765 \cdot 10^{16}$	$-0.34254 \cdot 10^{15}$	$0.14349 \cdot 10^{15}$
$1 \cdot 10^{-09}$	$0.72230 \cdot 10^{20}$	$-0.72411 \cdot 10^{20}$	$0.19462 \cdot 10^{18}$	$-0.11460 \cdot 10^{17}$	$0.16576 \cdot 10^{16}$
$1 \cdot 10^{-10}$	$0.23404 \cdot 10^{23}$	$-0.23423 \cdot 10^{23}$	$0.19328 \cdot 10^{20}$	$-0.36984 \cdot 10^{18}$	$0.17408 \cdot 10^{17}$
$1 \cdot 10^{-11}$	$0.74605 \cdot 10^{25}$	$-0.74624 \cdot 10^{25}$	$0.19283 \cdot 10^{22}$	$-0.11785 \cdot 10^{20}$	$0.17784 \cdot 10^{18}$
$1 \cdot 10^{-12}$	$0.23654 \cdot 10^{28}$	$-0.23656 \cdot 10^{28}$	$0.19271 \cdot 10^{24}$	$-0.37471 \cdot 10^{21}$	$0.15894 \cdot 10^{19}$

Therefore, numeric evaluation of the asymptotic behavior of the RC cross section at small Q^2 can require an unprecedented accuracy of integration over the real photon phase space.

Asymptotics of specific Contributions: Summary

The final formulas for the leading $q_m = Q/m$ asymptotic, i.e., in the approximation $Q^2 \ll m^2 \ll S, M^2$ are

$$\frac{d\sigma_{obs}}{dQ^2} = \exp\left(\frac{\alpha}{\pi}\delta_{inf}\right)\left[1+\frac{\alpha}{\pi}\delta\right]\frac{d\sigma_B}{dQ^2} + \frac{d\sigma_F}{dQ^2}.$$

where

- Born cross section is proportional to Q^{-4}

$$\frac{d\sigma_B}{dQ^2} = \frac{4\pi\alpha^2}{Q^4}G_e^2(0)$$

- Infrared-free cross section of the photon radiation is proportional to Q^{-2}

$$\frac{d\sigma_F}{dQ^2} = -\frac{\alpha^3}{\pi Q^2 m^2}\left(\frac{19}{9}-\frac{2}{3}L_s\right)G_e^2(0)$$

- factorized correction δ_{inf} and δ are:

$$\delta_{inf} = \frac{q_m^2}{3}\left(2\log q_m + L_s\right) \qquad and \qquad \delta = \frac{q_m^2}{6}\left(\frac{23}{10} - L_s\right)$$

Numeric illustrations

Q^2, GeV^2	Born nb GeV^{-2}	δ_{VR}^{max}	δ_{VR}^{cut}	RC_F^{max}	RC_F^{cut}
$1 \cdot 10^{-8}$	$0.41 \cdot 10^{18}$	-0.0001	-0.0006	0.0003	$-0.12 \cdot 10^{-8}$
$1 \cdot 10^{-7}$	$0.41 \cdot 10^{16}$	-0.0001	-0.0056	0.0023	$-0.12 \cdot 10^{-7}$
$1 \cdot 10^{-6}$	$0.41 \cdot 10^{14}$	0.0017	-0.0392	0.0111	$-0.82 \cdot 10^{-7}$
$1 \cdot 10^{-5}$	$0.41 \cdot 10^{12}$	0.0080	-0.1249	0.0265	$-0.30 \cdot 10^{-6}$
$1 \cdot 10^{-4}$	$0.41 \cdot 10^{10}$	0.0158	-0.2284	0.0305	$-0.56 \cdot 10^{-6}$
$1 \cdot 10^{-3}$	$0.41 \cdot 10^{8}$	0.0237	-0.3339	0.0247	$-0.17 \cdot 10^{-5}$
$1 \cdot 10^{-2}$	$0.40 \cdot 10^{6}$	0.0315	-0.4395	0.0181	$-0.68 \cdot 10^{-6}$

Q^2, GeV^2	RC_{AMM}	δ_{vac}^{l}	δ_{vac}^{h}	RC_{tot}^{max}	RC_{tot}^{cut}
$1 \cdot 10^{-8}$	$-0.75 \cdot 10^{-11}$	$0.14 \cdot 10^{-4}$	$0.18 \cdot 10^{-9}$	0.0003	-0.0006
$1 \cdot 10^{-7}$	$-0.71 \cdot 10^{-10}$	$0.11 \cdot 10^{-3}$	$0.18 \cdot 10^{-8}$	0.0024	-0.0055
$1 \cdot 10^{-6}$	$-0.48 \cdot 10^{-9}$	$0.87 \cdot 10^{-3}$	$0.18 \cdot 10^{-7}$	0.0137	-0.0383
$1 \cdot 10^{-5}$	$-0.14 \cdot 10^{-8}$	$0.33 \cdot 10^{-2}$	$0.18 \cdot 10^{-6}$	0.0378	-0.1216
$1 \cdot 10^{-4}$	$-0.23 \cdot 10^{-8}$	$0.67 \cdot 10^{-2}$	$0.18 \cdot 10^{-5}$	0.0530	-0.2218
$1 \cdot 10^{-3}$	$-0.32 \cdot 10^{-8}$	$0.10 \cdot 10^{-1}$	$0.18 \cdot 10^{-4}$	0.0587	-0.3237
$1 \cdot 10^{-2}$	$-0.39 \cdot 10^{-8}$	$0.14 \cdot 10^{-1}$	$0.18 \cdot 10^{-3}$	0.0639	-0.4253

Numeric illustrations

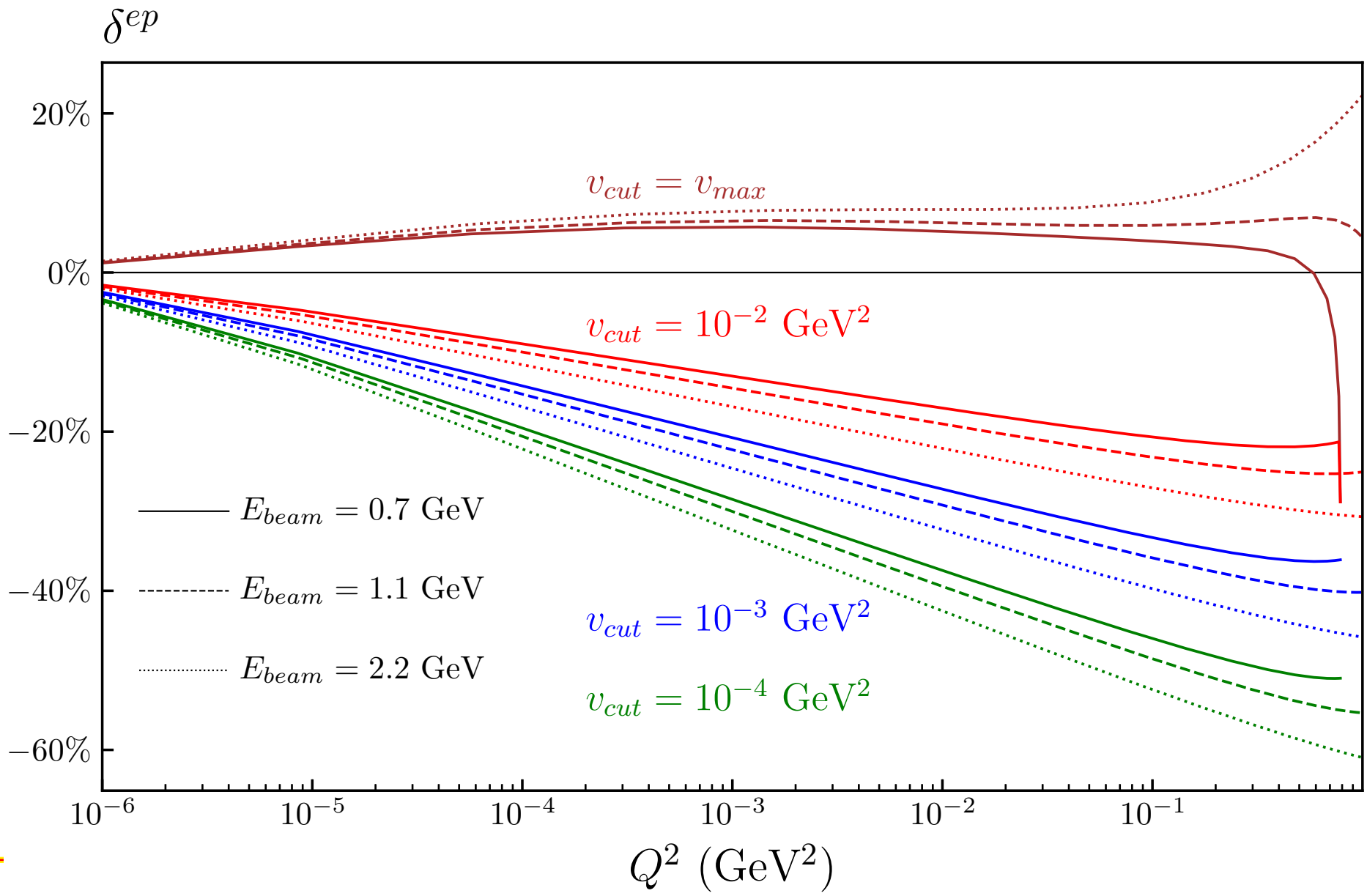

Møller scattering Feynman graphs

- Born matrix elements: t and u-channels

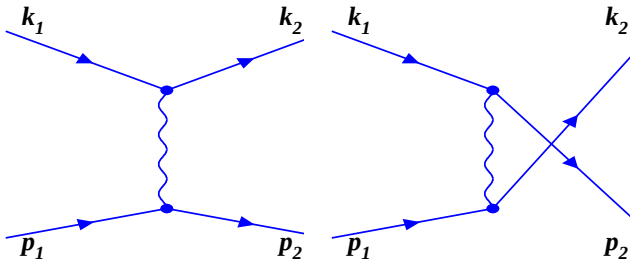

- Matrix elements of RC in the t-channel

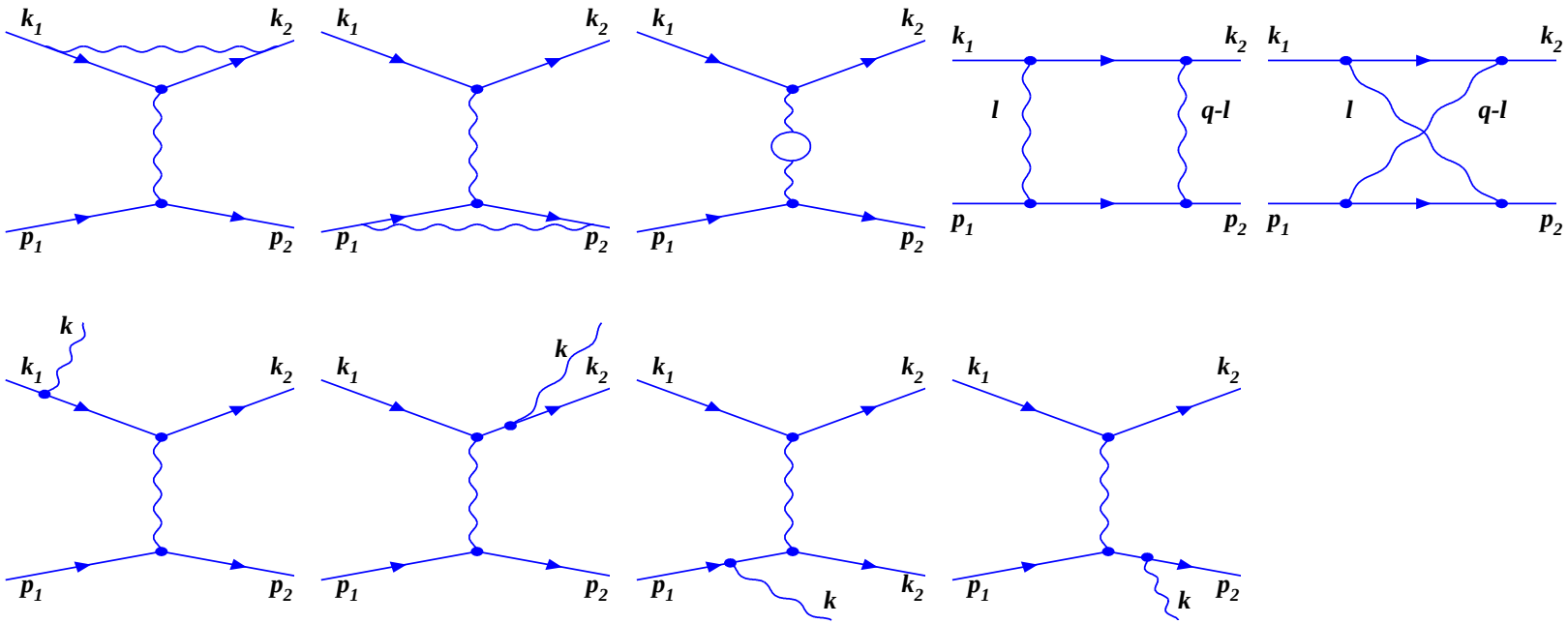

Møller scattering: Contributions to RC

Møller scattering

$$e^-(k_1) + e^-(p_1) \to e^-(k_2) + e^-(p_2)$$

is described in terms of Mandelstam variables

$$s = (k_1 + p_1)^2, \;\; t = (k_1 - k_2)^2, \;\; u = (p_1 - k_2)^2 = 4m^2 - s - t.$$

$$\frac{d\sigma_B}{dc_\theta} = \frac{d\sigma_B^t}{dc_\theta} + (t \leftrightarrow u),$$

where

$$\frac{d\sigma_B^t}{dc_\theta} = \frac{\mathcal{M}_b^t \mathcal{M}_b^+}{32\pi s} = \frac{\pi\alpha^2}{2s}\left[\frac{(s-u)^2 + t(t-8m^2)}{t^2} + 2\frac{(s-6m^2)(s-2m^2)}{tu}\right].$$

$$\frac{d\sigma_{RC}(v_{cut})}{dc_\theta} = \frac{d\sigma_{\rm virt}}{dc_\theta} + \frac{d\sigma_R}{dc_\theta} = \frac{\alpha}{\pi}\delta_{VR}\frac{d\sigma_B}{dc_\theta} + \frac{\alpha}{\pi}\left[\delta_{\rm virt}^t \frac{d\sigma_B^t}{dc_\theta} + \delta_{\rm virt}^u \frac{d\sigma_B^u}{dc_\theta}\right] + \frac{d\sigma_F}{dc_\theta}$$

$$+ \frac{d\sigma_{\rm AM}^t}{dc_\theta} + \frac{d\sigma_{\rm AM}^u}{dc_\theta} + \frac{d\sigma_{2\gamma d}^{t\;F}}{dc_\theta} + \frac{d\sigma_{2\gamma d}^{u\;F}}{dc_\theta} + \frac{d\sigma_{2\gamma x}^{t\;F}}{dc_\theta} + \frac{d\sigma_{2\gamma x}^{u\;F}}{dc_\theta},$$

Numeric illustrations

Q^2, GeV^2	Born nb GeV^{-2}	δ_{VR}	δ^t_{virt}	δ^u_{virt}	RC_F
$1 \cdot 10^{-8}$	$0.72 \cdot 10^{10}$	0.0005	0.0001	$-0.27 \cdot 10^{-06}$	-0.0004
$1 \cdot 10^{-7}$	$0.72 \cdot 10^{8}$	0.0047	0.0005	$-0.27 \cdot 10^{-05}$	-0.0036
$1 \cdot 10^{-6}$	$0.72 \cdot 10^{6}$	0.0324	0.0021	$-0.27 \cdot 10^{-04}$	-0.0238
$1 \cdot 10^{-5}$	$0.72 \cdot 10^{4}$	0.0999	-0.0050	$-0.27 \cdot 10^{-03}$	-0.0386
$1 \cdot 10^{-4}$	$0.72 \cdot 10^{2}$	0.1713	-0.0350	$-0.29 \cdot 10^{-02}$	0.0661
$1 \cdot 10^{-3}$	$1.42 \cdot 10^{0}$	0.2181	-0.0502	$-0.44 \cdot 10^{-01}$	0.4357
$2 \cdot 10^{-3}$	$3.42 \cdot 10^{1}$	0.1815	-0.0044	$-0.42 \cdot 10^{-01}$	0.1048

Q^2, GeV^2	RC^t_{AMM}	RC^u_{AMM}	δ_{box}	RC^{max}_{tot}	RC^{cut}_{tot}
$1 \cdot 10^{-8}$	$-0.25 \cdot 10^{-11}$	$0.36 \cdot 10^{-10}$	$-0.24 \cdot 10^{-05}$	0.0016	-0.0002
$1 \cdot 10^{-7}$	$-0.11 \cdot 10^{-10}$	$0.36 \cdot 10^{-09}$	$-0.13 \cdot 10^{-04}$	0.0156	-0.0014
$1 \cdot 10^{-6}$	$0.79 \cdot 10^{-09}$	$0.36 \cdot 10^{-08}$	$-0.63 \cdot 10^{-04}$	0.0107	-0.0090
$1 \cdot 10^{-5}$	$0.27 \cdot 10^{-07}$	$0.36 \cdot 10^{-07}$	$-0.24 \cdot 10^{-03}$	0.0562	-0.0279
$1 \cdot 10^{-4}$	$0.48 \cdot 10^{-06}$	$0.39 \cdot 10^{-06}$	$0.49 \cdot 10^{-04}$	0.2020	-0.0545
$1 \cdot 10^{-3}$	$0.47 \cdot 10^{-05}$	$0.46 \cdot 10^{-05}$	$0.93 \cdot 10^{-02}$	0.5789	-0.0875
$2 \cdot 10^{-3}$	$0.58 \cdot 10^{-06}$	$0.74 \cdot 10^{-06}$	$0.38 \cdot 10^{-02}$	0.2441	-0.0600

Numeric illustrations

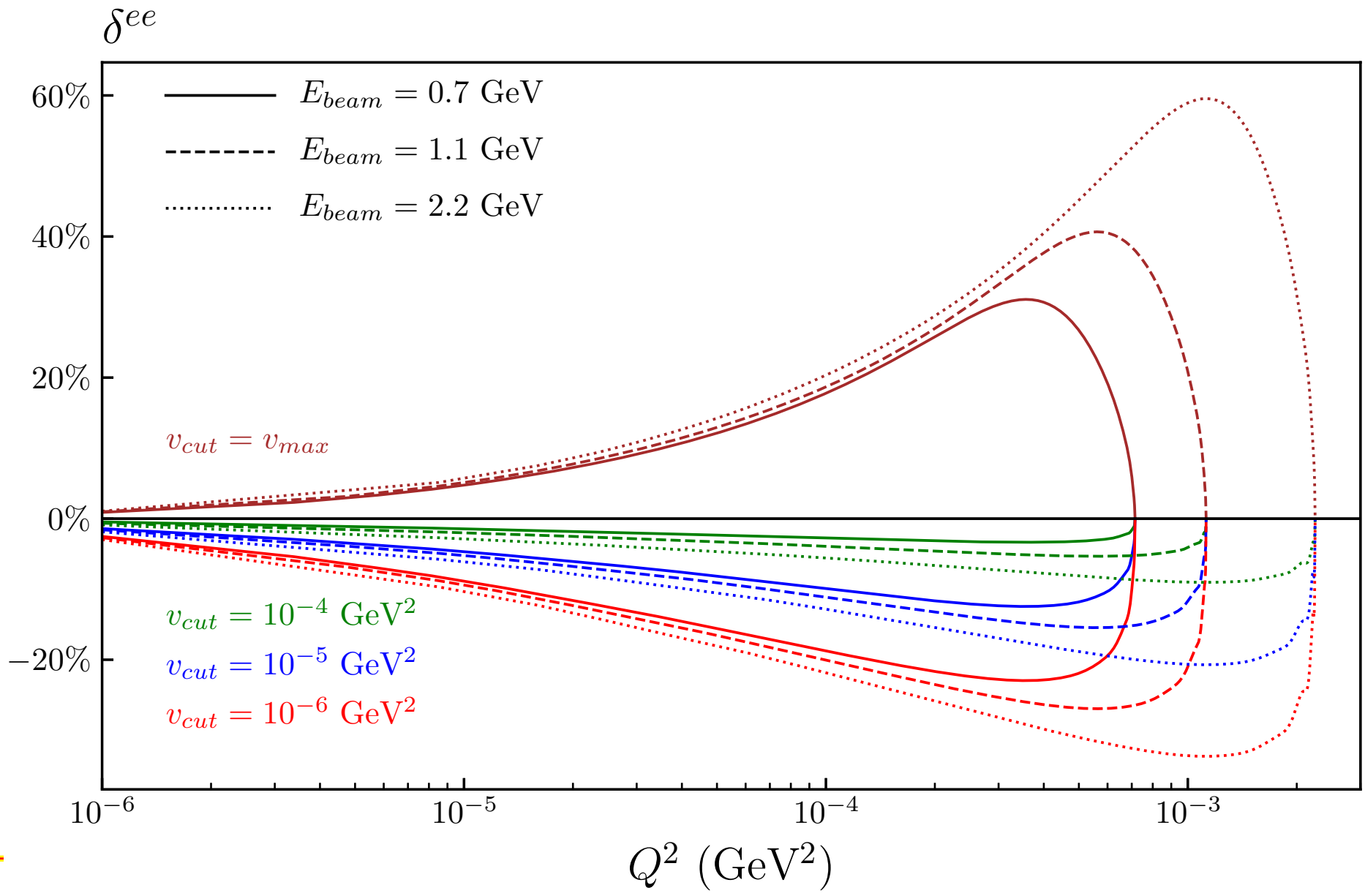

Possible contributions to at small Q^2

Consider t-channel box-type contributions in the approximation $-t \ll m^2 \ll s$

- Direct boxes:

$$\frac{2s\alpha^3}{t^2}\left(2L_sL_t - x_t(\pi^2 + (L_t-2)x_t\right) - \frac{\alpha^3}{t}\left(L_s - L_s^2 + 7L_t - 12 + \frac{4}{3}\pi^2\right)$$

- Cross boxes:

$$-\frac{2s\alpha^3}{t^2}\left(2L_sL_t - x_t(\pi^2 + (L_t-2)x_t\right) - \frac{\alpha^3}{t}\left(4L_sL_t + L_s - L_s^2 - 5L_t + 20 + \frac{1}{3}\pi^2\right)$$

- their sum

$$-\frac{2\alpha^3}{t}\left(2L_sL_t + L_s - L_s^2 + L_t + 4 + \frac{5}{6}\pi^2\right)$$

Here:

$$L_s = \log\left(\frac{s}{m^2}\right), \qquad L_t = \log\left(\frac{-t}{m^2}\right), \qquad x_t = \frac{\sqrt{-t}}{m}.$$

RC to the ep/ee ratio: additional properties

- The quantity of interest is R, the ratio of the cross sections for ep and ee scattering.
- RC to the ratio is:

$$\delta_R = \frac{R_{obs} - R_B}{R_B}$$

- The difference in the numerator is:

$$\frac{\sigma^{ep}_{obs}}{\sigma^{ee}_{obs}} - \frac{\sigma^{ep}_{B}}{\sigma^{ee}_{B}} = \frac{\sigma^{ep}_{B} + \sigma^{ep}_{RC}}{\sigma^{ee}_{B} + \sigma^{ee}_{RC}} - \frac{\sigma^{ep}_{B}}{\sigma^{ee}_{B}} \approx \frac{\sigma^{ee}_{B}\sigma^{ep}_{RC} - \sigma^{ep}_{B}\sigma^{ee}_{RC}}{\sigma^{ee}_{B}\sigma^{ep}_{B}} R_B = (\delta^{ep}_{RC} - \delta^{ee}_{RC})R_B$$

- Thus,

$$\delta_R = \delta^{ep}_{RC} - \delta^{ee}_{RC}$$

Therefore, the conclusion from this analysis is that if a contribution to RC is identical for the cross sections of ep and ee-scattering then this contribution does not contribute to RC to the ratio R.

Examples of such contributions are a factorized part of box diagrams, soft photon emission (from all lines), maybe some contributions of the higher orders.

Lessons from analysis of the small Q^2 asymptotics

- The Born contribution is of order $1/Q^4$
- The radiative correction is of order $1/(Q^2m^2)$
- The large logarithm is still available and contribute to RC as $L_s = \log\big(S/(mM)\big)$
- RC to the cross sections of ep and Møller scattering are similar
- Contributions to RC identical for ep and Møller scattering can be ignored when RC to the ratio is considered
- The resulting behavior $1/(Q^2m^2)$ for hard photon contribution is the result of exact analytical cancellation of specific terms of higher order in respect of Q^2, namely, terms of the order of $1/Q^3$, $1/Q^4$, and $1/Q^5$.
- The above behavior is obtained after analytic integration over the polar angle of the real photon momentum.
- These properties impose additional requirements to the approaches involving Monte Carlo integration over all photon variables at small Q^2.

The contributions to be studies: Box-type diagrams

Most popular approaches to evaluation of the two-photon exchange in ep-scattering include:

- approaches involving effective proton vertexes.
  - This approach approach approximates the two-photon exchange amplitude using a simplified hadronic model in which
  - the hadron is treated an elementary structureless fermion that interacts with the virtual photon through an effective coupling
  - adjustable photon-hadron coupling is described by a momentum-dependent effective vertex with phenomenological parameters (e.g., masses of resonances and various structure functions and form factors) fitted to medium-energy experimental data.
- approaches based on ideas of unitarity and involving disperse relations.
  - Using unitarity, the two-photon matrix element is approximated by inserting intermediate hadronic states with
  - the product of two electromagnetic currents with sums over intermediate hadronic states
  - This allows the process to be expressed in terms of known quantities: proton form factors for proton intermediate states and structure functions for hadronic states.

The implementation is in progress. Our preliminary estimates (interference of radiation by leptons and hadrons with the infrared part of boxes) show that the effect is not large and decrease with Q^2

The contributions to be studies: Box-type diagrams

Specifically, we calculated interference between

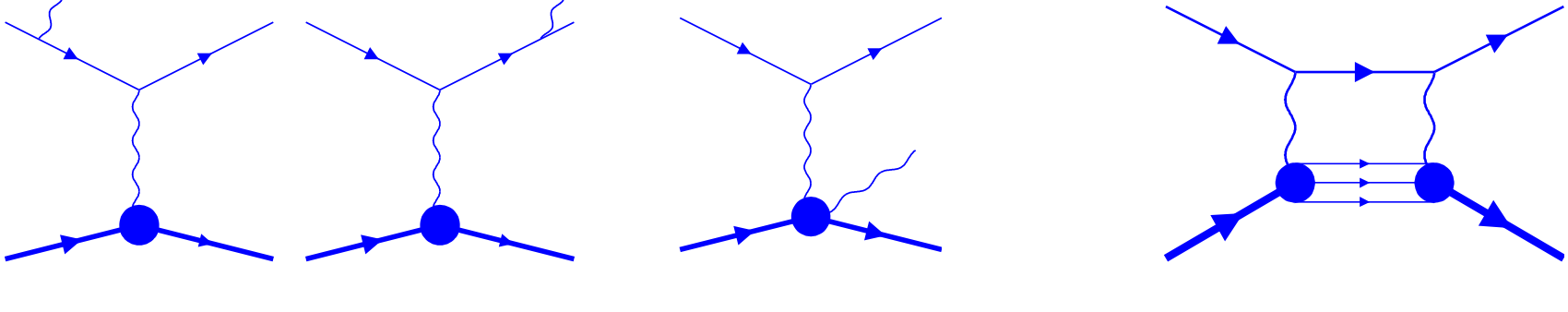

Further possible extensions:

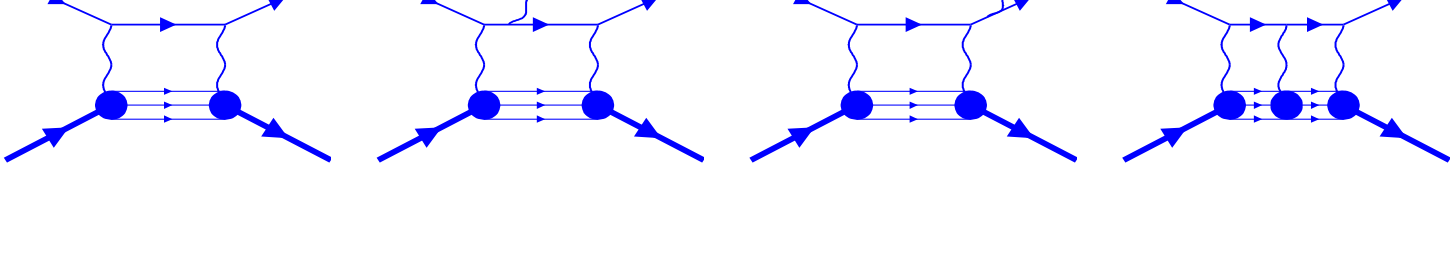

The contributions to be studies: Higher order effects

The second order effects for ep-scattering include four classes of diagrams with

- Two photons in the final state;
- A lepton-pair production;
- One loop effects with one photon in the final state;
- Two-loop effects.

Two photons in the final state:

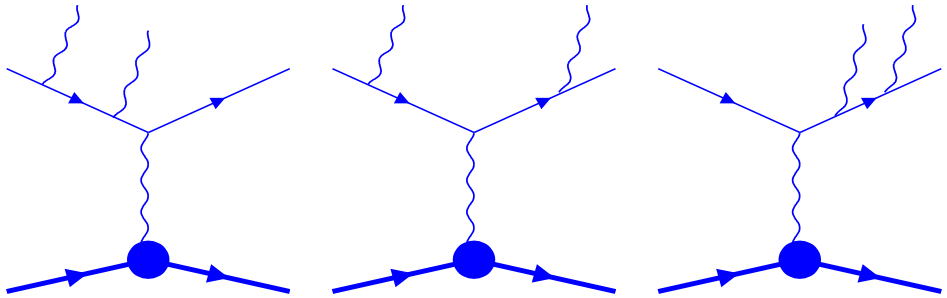

A lepton-pair production:

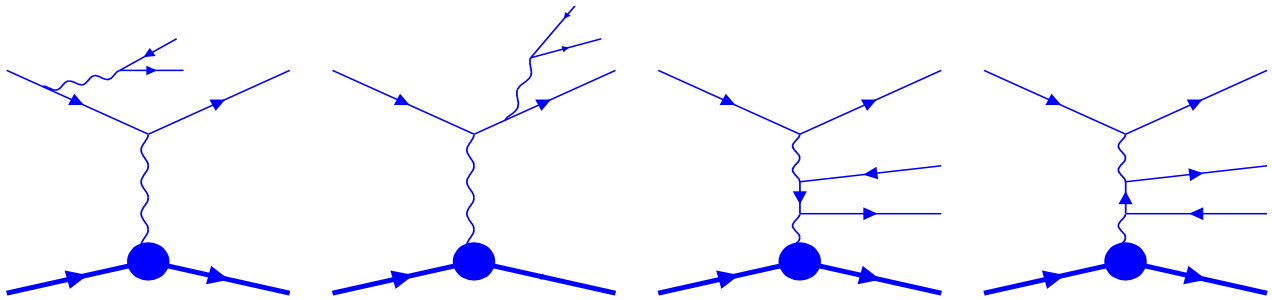

Higher order effects: Feynman graphs

One loop effects with one photon in the final state

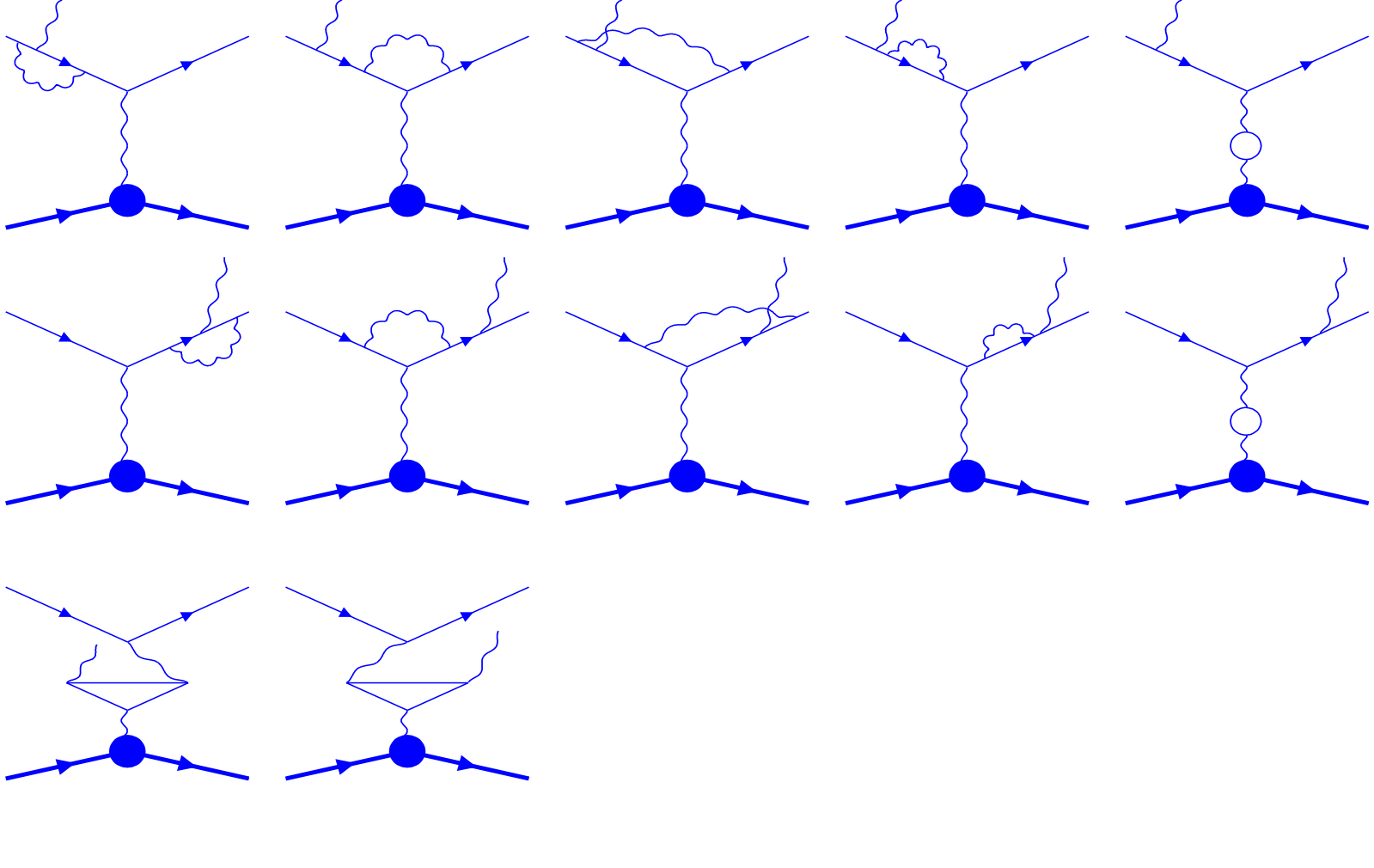

Higher order effects: Feynman graphs

Two-loop effects

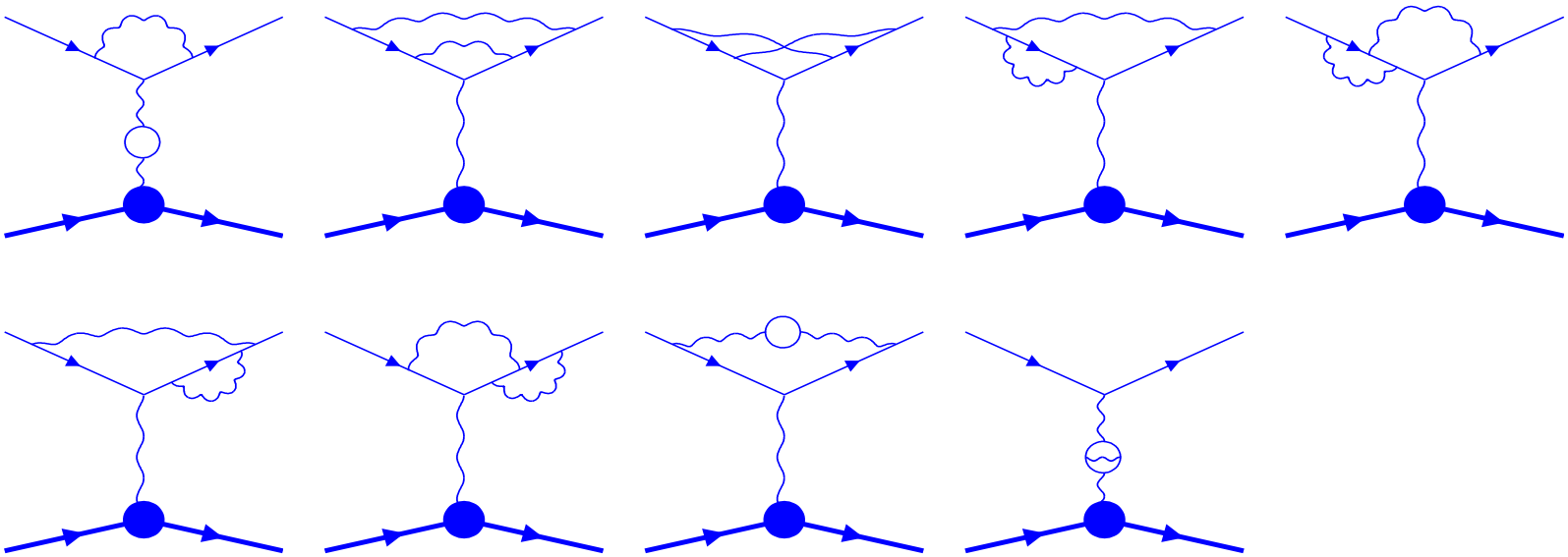

- The infrared divergence can be canceled only in the sum of the infrared divergence terms coming from the cross sections of the three processes (i., iii., and iv. classes) so they cannot be considered separately.
- Another problem is evaluation of finite parts that comes from i) integration over the phase space of radiated hard photons or lepton pairs and ii) two-loop contributions. In both cases the calculations require multidimensional integration.

Higher order effects: Approaches

Three levels of evaluating effects of a higher order (NNLO):

- Calculate exactly: not feasible from our point of view;
- Calculate with one or several alternative approximations;
- Estimate the contribution of NNLO to the systematic error due to RC

Our approach involves:

- Extension of our calculation for DVCS (Phys. Rev. D, 90(3):033001, 2014) in combination of one of the approach for two-loop calculation.
- Comparison with the results of analytic calculation performed by other groups (e.g., Drs. Hubert Spiesberger, and/or Aleksandrs Aleksejevs).
- Comparison with the results provided by the code McMule.
- Evaluation the contribution of NNLO to the systematic error due to RC using multiple soft photons and the method of structure functions.

An additional note:

- The contribution of the higher order RC to the systematic error can be estimated by comparison of the observed distribution of the cross section vs. v_{cut} with predictions given by mulple soft photon emission ot the method of electron structure functions.

Why the method of ESF can work

- *The QED radiative corrections to the corresponding cross sections can be written as a contraction of two electron structure functions and the hard part of the cross section.*

- *Traditionally, these radiative corrections include effects caused by loop corrections and soft and hard collinear radiation of photons and e+e- pairs.*

$$\sigma^{in} = \int_{z_1^m}^{1} dz_1 D(z_1, Q^2) \int_{\hat{z}_2^m}^{1} \frac{dz_2}{z_2^2} D(z_2, Q^2) \sqrt{\frac{\hat{\lambda}_Y}{\lambda_Y}} \frac{S_x^2}{\hat{S}_x^2} \hat{\sigma}_t^B$$

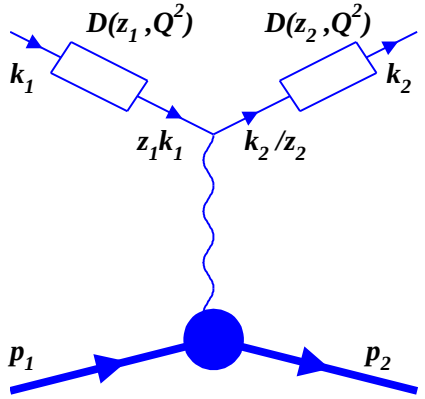

with ESF $D(z_{1,2}, Q^2) = D^{\gamma}(z_{1,2}, Q^2) + D_N^{e+e-}(z_{1,2}, Q^2) + D_S^{e+e-}(z_{1,2}, Q^2)$ *(e.g., Journal of Experimental and Theoretical Physics, 98(3) 403-416).*

Application of ESF to PRad kinematics requires modifications for the region

$$Q^2 \ll m^2 \ll S, M^2$$

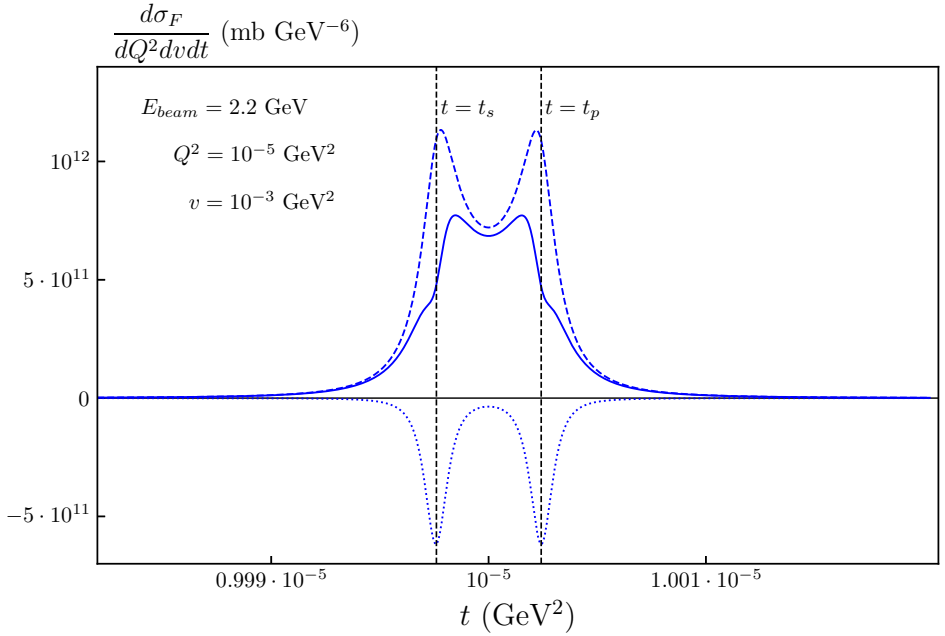

.

Conclusions

- Radiative corrections in PRad kinematics are on partial control:
  - The lowest order RC is calculated using alternative approaches, and comparison between their predictions is in progress.
  - Both total RC and specific contributions go down with decreasing Q^2.
  - Important property is that the actual result for RC due to hard photon emission is obtained through mutual cancellation of specific contributions with large effects of higher orders in respect of $1/Q^2$.
  - Further comparison among alternative approaches are still required.
- Radiative correction at higher order (NNLO) requires further efforts.
  - Progress is possible based on the results of mutual comparison of the calculations obtained using methods involving analytic integration (e.g., our group) and approaches involving numeric/Monte Carlo integration over the entire phase space (e.g., McMule group).
  - The systematic error due to NNLO effects can be studied using multiple soft photons and electron structure functions in comparison with actual experimental data for different inelasticity cuts.